Transcript and protein profiling identifies signaling, growth arrest, apoptosis, and NF-κB survival signatures following GNRH receptor activation

Colette Meyer, Andrew H Sims, Kevin Morgan[1],*, Beth Harrison, Morwenna Muir, Jianing Bai, Dana Faratian, Robert P Millar[2,3] and Simon P Langdon

Breakthrough Breast Cancer Research Unit and Division of Pathology, Institute of Genetics and Molecular Medicine, University of Edinburgh, Crewe Road South, Edinburgh EH4 2XU, UK
[1]Medical Research Council Human Reproductive Sciences Unit, Queen's Medical Research Institute, 47 Little France Crescent, Edinburgh EH16 4TJ, UK
[2]Centre for Integrative Physiology, University of Edinburgh, Edinburgh EH8 9XD, UK
[3]Mammal Research Institute, University Pretoria, and UCT/MRC Receptor Biology Unit, University of Cape Town, Cape Town, South Africa
*K Morgan is now at Respiratory Medicine, University of Hull, Hull, UK

Correspondence should be addressed to S P Langdon
Email
simon.langdon@ed.ac.uk

Abstract

GNRH significantly inhibits proliferation of a proportion of cancer cell lines by activating GNRH receptor (GNRHR)-G protein signaling. Therefore, manipulation of GNRHR signaling may have an under-utilized role in treating certain breast and ovarian cancers. However, the precise signaling pathways necessary for the effect and the features of cellular responses remain poorly defined. We used transcriptomic and proteomic profiling approaches to characterize the effects of GNRHR activation in sensitive cells (HEK293-GNRHR, SCL60) in vitro and in vivo, compared to unresponsive HEK293. Analyses of gene expression demonstrated a dynamic response to the GNRH superagonist Triptorelin. Early and mid-phase changes (0.5–1.0 h) comprised mainly transcription factors. Later changes (8–24 h) included a GNRH target gene, CGA, and up- or downregulation of transcripts encoding signaling and cell division machinery. Pathway analysis identified altered MAPK and cell cycle pathways, consistent with occurrence of G_2/M arrest and apoptosis. Nuclear factor kappa B (NF-κB) pathway gene transcripts were differentially expressed between control and Triptorelin-treated SCL60 cultures. Reverse-phase protein and phospho-proteomic array analyses profiled responses in cultured cells and SCL60 xenografts in vivo during Triptorelin anti-proliferation. Increased phosphorylated NF-κB (p65) occurred in SCL60 in vitro, and p-NF-κB and IκBε were higher in treated xenografts than controls after 4 days Triptorelin. NF-κB inhibition enhanced the anti-proliferative effect of Triptorelin in SCL60 cultures. This study reveals details of pathways interacting with intense GNRHR signaling, identifies potential anti-proliferative target genes, and implicates the NF-κB survival pathway as a node for enhancing GNRH agonist-induced anti-proliferation.

Endocrine-Related Cancer

Introduction

GNRH analog therapy is used in the treatment of hormone-dependent cancers, such as prostate and breast cancers, to suppress androgen and estrogen production. In addition, GNRH agonists and antagonists have direct anti-proliferative effects (independent of their hormone regulatory actions) on various reproductive tissue cancer cell lines from prostate (Limonta et al. 1992, 2012, Moretti et al. 1996, Angelucci et al. 2004, Morgan et al. 2011a), breast (Blankenstein et al. 1985, Miller et al. 1985, Eidne et al. 1987, Marini et al. 1994, Emons et al. 2003, Finch et al. 2004), ovary (Emons et al. 1989, 1993b, Grundker et al. 2000, 2001, 2002, Maudsley et al. 2004), and endometrium (Emons et al. 1993a, Grundker et al. 2001, 2002, Acharya et al. 2008). Depending on the cellular phenotype, intense signaling from activated GNRH receptor (GNRHR) can induce cell cycle arrest in G_2, with or without concomitant induction of apoptosis. The activated receptor couples to Gq/11 and elicits rapid transient phospholipase C activation, mobilization of intracellular calcium (via inositol trisphosphate (IP_3)), protein kinase C activation (via diacylglycerol (DAG)) and activation of MAP kinase, and stress-activated kinase signaling (ERK, JNK, and p38) (Morgan et al. 2008). A role for Gi has been proposed by various investigators but has yet to be critically tested beyond the application of pertussis toxin in co-treatment assays and this contrasts with a crucial role for Gq/11(White et al. 2008).

Although inappropriate signaling results in cellular stress, the details concerning how this stress is converted into a commitment to growth arrest and/or apoptosis are largely uncharacterized. The cellular response is likely to be complex, with changes in gene transcription and regulation of proteins affecting functions of key importance to cell fate. More details concerning the response to GNRHR activation are required in order to understand the anti-proliferative mechanism and to explain why certain cells are more sensitive than others, even though they express similar levels of GNRHR (Morgan et al. 2008). A high level of GNRHR expression at the cell surface correlates with responsiveness to GNRH (Morgan et al. 2008), supporting the hypothesis that there is a requirement for direct interaction between GNRHR and agonist at the cell surface. Identifying the determinants of sensitivity to GNRH analogs would potentially allow sensitive tumors to be selected for treatment.

In order to identify signaling factors required for response to the potent GNRH superagonist, Triptorelin, we employed transcript profiling and protein array analysis of the model human HEK293 (SCL60) cells in vitro and in tumor xenografts to identify markers likely to reflect the anti-proliferative mechanism. This model is a HEK293 cell line transfected with a high level of the GNRHR (Morgan et al. 2008). In most published studies of cancer cells, the presence of GNRHR is inferred on the basis of RT-PCR detection of mRNA and/or by detection of ligand binding to whole cell lysates. In those instances, detection of GNRHR mRNA cannot reliably indicate how much functional GNRHR is present and ligand binding assays usually need to be pushed to the limit of detection sensitivity to infer specific GNRH analog binding. Using HEK293 cells transfected to overexpress GNRHR circumvents these problems and direct comparison can be made to wild-type HEK293 cells. The utility of transfected cell studies has been re-iterated recently (Morgan et al. 2011b).

Our strategy extends preliminary data generated using mouse pituitary tumor LβT2 (White et al. 2008), which serves as a useful benchmark comparison (Morgan et al. 2008). We discovered dynamic changes in gene transcription and altered protein phosphorylation in pathways, which shed more light on the anti-proliferative mechanism of GNRHR activation, and suggest ways in which its effectiveness may be improved.

Materials and methods

Cell lines

SCL60 cells are HEK293 cells stably transfected with a high level of functional rat GNRHR (Morgan et al. 2008). SCL60 cells express surface levels of GNRHR similar to that of GNRHR at the surface of mouse embryo pituitary gonadotrope cell line LβT2 (White et al. 2008). This level is similar to that found in mature pituitary gonadotrope cells and at least 100-fold higher than surface receptor levels in any cancer cell line thought to express endogenous GNRHR (Morgan et al. 2008, 2011a).

SCL215 cells stably express a rat GNRHR fused to a catfish GNRHR C-terminal cytoplasmic domain (under G418 selection). The fusion protein binds GNRH analogs, but this does not activate signaling.

HEK293, SCL60, and SCL215 cells were cultured in DMEM with 10% fetal bovine serum. SCL60 and SCL215 cells were supplemented with G418 antibiotic (0.5 mg/ml). For all these cell lines, tissue culture plates were coated with a diluted Matrigel solution (200 μl Matrigel (BD Biosciences, Oxford, UK) per 6 ml DMEM media, 22 °C for 1–2 h, excess removed before adding cells) to assist cell adherence. Cell doubling times for each of the cell lines in basal conditions are similar ($\sim$22 h).

In vitro gene expression profiling

SCL60 or HEK293 cells were treated with 100 nM Triptorelin (Sigma), or an appropriately diluted 20% propylene glycol (Sigma) solution (final concentration: 0.02% propylene glycol). RNA was isolated at 0, 0.5, 1, 2, 8, and 24 h after treatment from four independent experiments on different days using the Absolutely RNA Miniprep kit (Stratagene, Leicester, UK) according to the manufacturer's instructions. Purified RNA was biotin labeled using the Illumina TotalPrep RNA Amplification Kit (Ambion, Huntingdon, UK) according to the manufacturer's instructions. Labeled RNA was hybridized to Illumina HT12 BeadChips and scanned at the Wellcome Trust Clinical Research Facility, Western General Hospital, Edinburgh. The gene expression data have been submitted to NCBI's Gene Expression Omnibus and is accessible through GEO Series accession number GSE27467. Gene expression analysis was performed using the open source statistical programming language, R (Ihaka & Gentleman 1996), and associated Bioconductor packages (Gentleman et al. 2004). Data were filtered to remove unreliably detected probes and one outlier replicate and then quantile-normalized using the Beadarray (Dunning et al. 2007) package. Differential expression was determined using Rank Products analysis (Breitling et al. 2004) with 5% false discovery rate.

Flow cytometric DNA analysis

Cells were treated with Triptorelin (100 nM) or 0.02% propylene glycol solution (vehicle control) for up to 72 h before being trypsinized, pelleted, and resuspended in pH 7.6 citrate buffer. Samples were stored at $-20\,°C$ until analysis and were then thawed to room temperature. The cells were incubated at room temperature with 0.003% trypsin solution (450 µl; 0.003% trypsin, 3.4 mM tri-sodium citrate, 0.1% NP40, 1.5 mM spermine hydrochloride, and 0.5 mM Tris base) for 2 min with agitation and then with a second solution (375 µl; 0.05% trypsin inhibitor, and 0.01% w/v RNase A) for 10 min. Finally, cells were treated with 250 µl propidium iodide solution (416 µg/ml propidium iodide, 1.16 mg/ml spermine tetrahydrochloride solution) on ice and in the dark for 10 min. The samples were analyzed using a BD FACSAriaII SORP Flow Cytometer (Becton Dickinson, Oxford, UK) and BD FACSDiva software (Becton Dickinson, Version 6.1.2).

Xenograft tumors

Tumors were derived from the GNRHR-transfected HEK293 cell line, SCL60, by s.c. bilateral implantation of these cells into the flank of athymic nude female mice (Morgan et al. 2008). Nine mice with 11 tumors were treated with Triptorelin (10 µg/mouse, 0.1 ml). Ten mice with 12 tumors were injected with a 20% propylene glycol solution (0.1 ml). Treatment was initiated when tumors were 50–100 mm³ in size. Xenograft material was collected at days 4 and 7 after treatment.

Phosphoprotein antibody array

Samples from three tumors following treatment with Triptorelin at day 4 and 7, along with six corresponding controls, were analyzed using the V250 antibody array (Eurogentec Ltd., Southampton, UK). This array comprises 117 pairs of antibodies to detect phosphorylated and non-phosphorylated forms of proteins that are typically dysregulated in cancer-related signaling. A full list of antibodies used is shown in Supplementary Table 1, see section on supplementary data given at the end of this article. Binding of each antibody to its target results in an emission fluorescence, whose intensity is proportional to the level of the target protein. The intensity score for each phosphorylated protein was normalized by Eurogentec Ltd. to that of its non-phosphorylated counterpart.

Immunohistochemistry

A tissue microarray (TMA) was constructed with five Triptorelin-treated and six untreated SCL60 xenografts in biological triplicate as described previously (Kononen et al. 1998). Hydrated TMA sections were incubated with primary antibody (rabbit anti-Cleaved Caspase 3 (Asp175; 1:100), rabbit anti-Phospho-Histone H3 (Ser10; 1:200), anti-nuclear factor kappa B (NF-κB) (1:00, Cell Signaling), or anti-pNF-κB (1: Cell Signaling, Hitchin, UK) for 1 h at room temperature and were detected via DakoCytomation envision/HRP Kit (K4003) (Dako, Ely, Cambridgeshire, UK). Finally, all the slides were counterstained in hematoxylin for 20 s, dehydrated, and mounted. After staining, slides were observed by $400\times$ magnification and a histoscore per core per slide was calculated.

Reverse-phase protein array

Protein was isolated from SCL60, HEK293, and SCL215 cells following treatment with Triptorelin (100 nM) or control for 0, 0.5, 1, 2, 4, 8, or 24 h from three independent experiments. Samples were diluted to 2 mg/ml and then twofold serially diluted to produce five dilutions of each sample. Each dilution was spotted (Spurrier et al. 2008) in

triplicate onto each pad of a 2-pad FAST nitrocellulose-coated glass slide (Whatman, Lutterworth, UK) using a BioRobotics Microgrid (Isogen Life Science, De Meern, The Netherlands). Samples were carefully distributed over the pads to ensure that a balance of control and treated samples was spotted by each pin. Slides were blocked with PBS:Li-Cor Blocking Buffer (1:1, 1 h RT) before incubation with primary antibody (overnight 4 °C). Phosphoprotein (p) expression was measured and compared with total (t) levels of expression.

Primary antibodies were Rabbit polyclonal, from Cell Signaling Technology UK, and diluted 1:50 unless otherwise stated: Anti-P21 (mouse, 1:150), anti-tPTEN (mouse, 1:300), anti-pPTEN (Ser80/Thr382/383), anti-tmTOR (1:300), anti-pmTOR (Ser2448), anti-tCDK2, anti-pCDK2, anti-tAKT (mouse, 1:1000), anti-pAKT (Ser473), anti-tNF-κB, anti-pNF-κB (Ser529), anti-tCyclinD1 (mouse, 1:300), anti-pCyclinD1 (Thr286), Ki67 (Dako, mouse, 1:250), anti-P38 (1:100), anti-pP38 (1:100), pHistone H3 (Ser10, 1:100), PI3K p110α (1:133), pERα (mouse, 1:100), tERα (Neomarkers, Maybridge, Tintagel, UK; 1:250), tCAV1, pCav1 (Tyr14), pMet (Tyr1349), tMet (mouse), pCHK2 (Ser516), tERK (Thr 202/204 for ERK1 and Thr 185/187 for ERK2) (mouse), pERK (1:100), P53 (mouse), and GNRHR (Leica, mouse). Slides were washed with PBS–0.1%Tween 20 (3×5 min) before applying secondary antibody diluted in Li-Cor blocking buffer (45 min RT, dark). The slides were washed in the dark with PBS–0.1% Tween 20 (3×5 min), PBS (3×5 min), and then dried at 50 °C. The slides were scanned on a Li-Cor Odyssey scanner at 680 and 780 nm. The image was analyzed using MicroVigene RPPA Analysis module software (VigeneTech, Carlisle, MA, USA). The means of the triplicate dilutions are used to produce a curve for each sample. The y-intercept is used as a relative measure of protein concentration between curves. This quantitative measurement is used in further analysis. Measurements for phosphoproteins were normalized to the corresponding total protein except for Ki67 and pHH3.

Cell growth assays

SCL60 cells were seeded into 12-well plates at 1×10^6 cells/ml. After 48 h, the cells were washed in serum-free media and then treated with 3 μM 15d-PGJ$_2$ (NF-κB inhibitor) or vehicle control (dimethyl sulfoxide) in serum-free media for 30 min before addition of 100 nM Triptorelin or vehicle control (final concentration: 0.02% propylene glycol) in complete media with serum. After 4 days, cell growth was measured by sulforhodamine B assay as described previously (Skehan et al. 1990).

Results

GNRHR activation induces S phase and G$_2$/M arrest in GNRHR-expressing cells in vitro

Triptorelin elicited 63% inhibition of SCL60 cell growth after 5 days of treatment but did not affect growth of untransfected parental (HEK293) cells or those transfected with an inactivating mutant GNRHR (SCL215) (Fig. 1A). Flow cytometric analysis of the cells demonstrated that the anti-proliferative effect of Triptorelin in SCL60 cells was associated with an accumulation of cells in the S and G$_2$/M phases of the cell cycle at 24 and 48 h after treatment compared with vehicle-treated control cells (Fig. 1B; Supplementary Figure 1, see section on supplementary data given at the end of this article). There was a significant increase in cleavage of the caspase-mediated apoptosis marker poly (ADP-ribose) polymerase (PARP; Fig. 1C). This increase was small after 48-h treatment with Triptorelin but was much more pronounced after 72–96 h (Fig. 1C). These results reproduce reported results for SCL60 cells (Morgan et al. 2008, 2011a).

Differential gene expression between GNRHR-expressing (SCL60) and parental (HEK293) cells

To explore the baseline differences in GNRHR-mediated signaling between these responsive and nonresponsive cell lines, we compared the global gene expression profile of the GNRHR-expressing SCL60 cell line with the parental cell line, HEK293. Over 4700 probes were consistently differentially expressed between replicate cultures of these cell lines (∼18% of detected probes on the microarray) using Rank Products analysis with 5% false positive rate). Genes that had higher expression in the GNRHR-expressing cells included genes involved in adhesion (CD44 and TACSTD1 (EPCAM)) and transcriptional regulation (SOX11, TCEAL3, and RUNX3), while genes that had significantly lower expression in SCL60 cells compared with HEK293 cells encoded many transcription regulators (including seven zinc finger proteins) and several proteins involved in adhesion (PCDH17, PCDH10, and SH3PXD2A) (Supplementary Table 1).

Dynamic transcriptional response to GNRHR activation in vitro

We next assessed the effect of Triptorelin treatment on gene expression in SCL60 cells before (0) and 0.5, 1, 2, 8, and 24 h after treatment. The greatest number of

differentially expressed genes (>1000) occurred after 8 h treatment with Triptorelin (Fig. 2A), with a higher proportion of genes upregulated rather than downregulated at the early time points (0.5–2 h). Downregulated
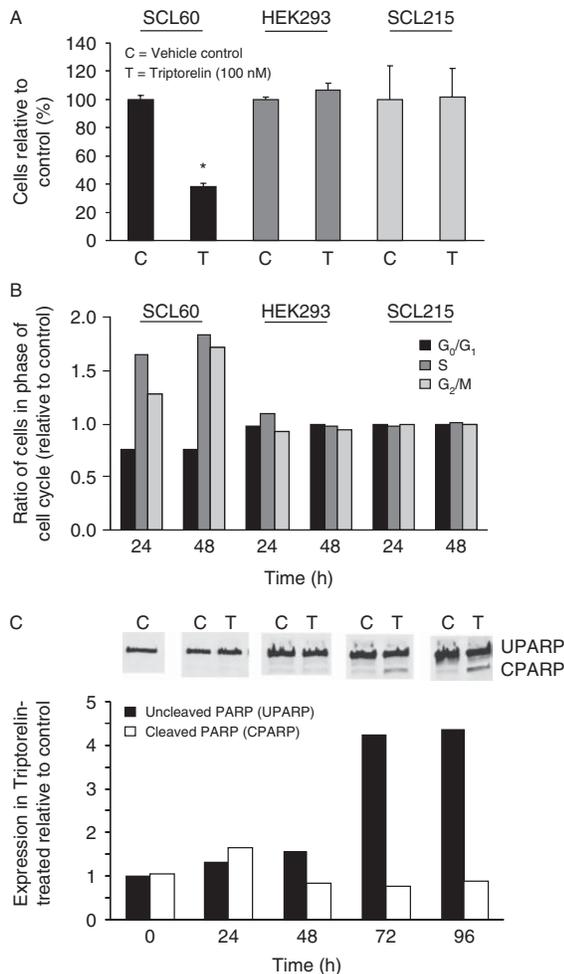

Figure 1

GNRH agonists reduce cell growth by cell cycle arrest and apoptosis *in vitro*. (A) Cell growth measured by sulforhodamine B assay following treatment with Triptorelin (100 nM) or vehicle control (0.02% propylene glycol) for 5 days. Bars show mean of three replicates. Error bars show S.D., *$P<0.01$. (B) Flow cytometric cell cycle analysis of SCL60, HEK293, and SCL215 cell lines following treatment with Triptorelin (100 nM) or vehicle control (0.02% propylene glycol) demonstrates that the anti-proliferative effect is characterized by cell cycle arrest. Data are expressed as a ratio of cells in each cell cycle phase, after Triptorelin treatment, relative to vehicle control samples. P values (paired t-test) for SCL60 triptorelin-treated vs control groups at 24 and 48 h are G_0/G_1 phase, $P=0.025$; S phase, $P=0.027$; and for G_2/M phase, $P=0.015$. (C) Western blot for caspase-mediated apoptosis marker-cleaved PARP. Values for Triptorelin-treated samples are shown relative to the corresponding vehicle control-treated samples at each time point (black bars). Uncleaved PARP expression is also shown (white bars). The lanes of the blot alternately show control and treated samples for each time point respectively. N.B. Control and treated at the zero time point are the same.
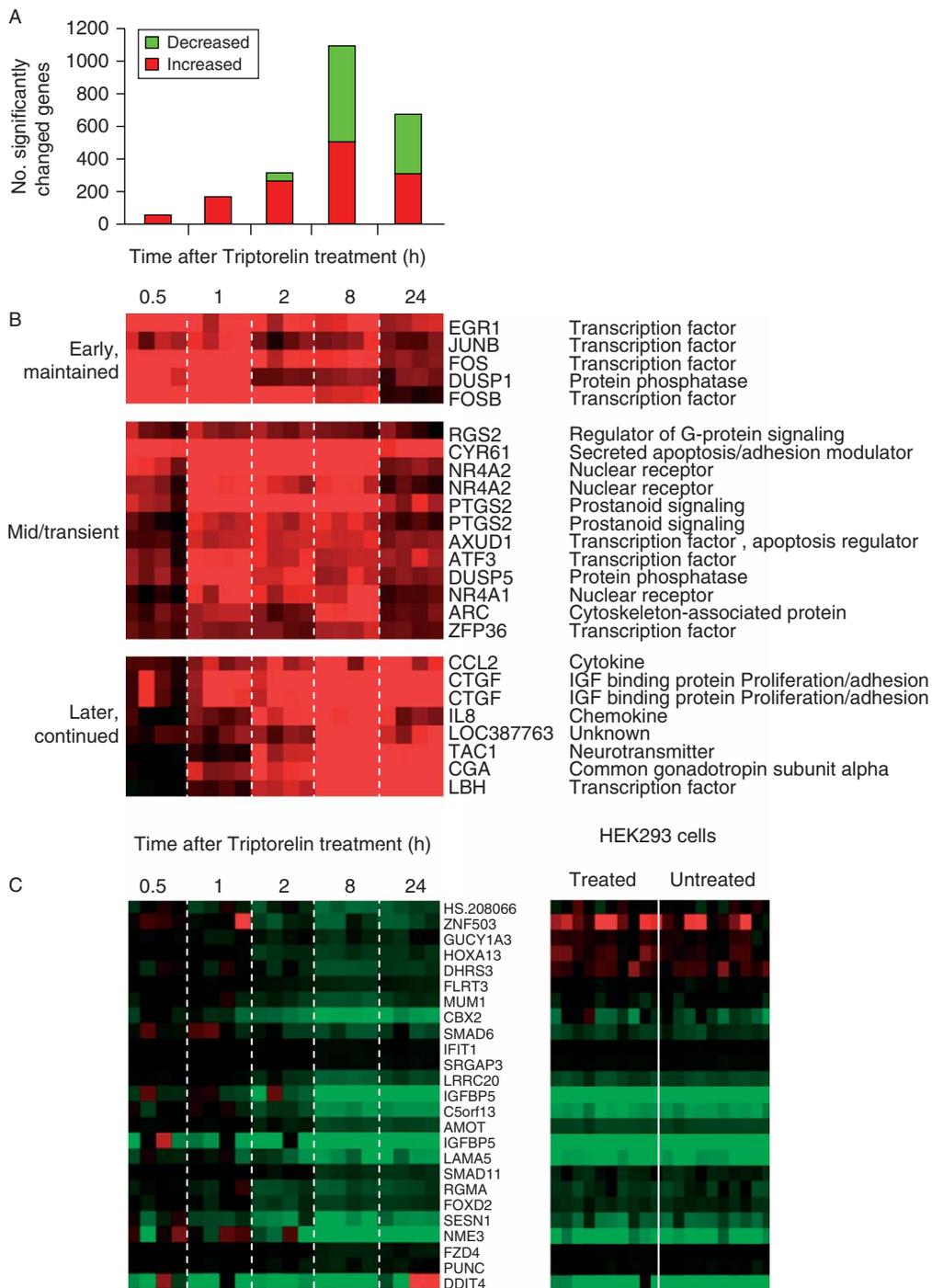
genes were more apparent after 2 h, presumably reflecting a secondary response, influenced in part by the primary response. The online pathway annotation tool, DAVID (Huang da *et al.* 2009), was used to determine which pathways were significantly enriched among the genes differentially expressed between SCL60 control and treated cells. Genes that were increased following treatment represented components of the cell cycle, MAPK and p53 signaling pathways, whereas transcripts that were decreased included cell cycle genes (Table 1). Clustering the most strongly upregulated genes in response to Triptorelin treatment in SCL60 cells showed at least three clusters of temporal expression (Fig. 2B). The 'early genes' (0.5–1 h) included early growth response 1 (*EGR1*), the MAP kinase inactivator DUSP1 (*MKP1*), along with the transcription factors JUNB, FOS, and FOSB (Fig. 2B). Genes that were increased later (8–24 h) included the epithelial cell stress chemokine, IL8, and the glycoprotein common gonadotropin subunit alpha (*CGA*), a GNRH signaling target gene in pituitary gonadotrope cells (Fig. 2B). The most downregulated genes included the cell motility SLIT-ROBO Rho GTPase activating protein SRGAP3, and the growth factor modulator IGF binding protein 5 (Fig. 2C). These genes were also mostly lower in HEK293 cells compared with SCL60-untreated cells but were unaffected by Triptorelin treatment in HEK293 cells (Fig. 2C). Of the genes that were significantly higher in SCL60 cells compared with HEK293 cells, 138 were also consistently increased with Triptorelin treatment in SCL60 cells, while 82 genes were downregulated after treatment and higher in SCL60 cells compared with HEK293 cells, including fibroblast growth factor receptor (*FGFR*) and *CACN* (involved in calcium channel formation). Pathways associated with these genes included MAPK and cell cycle signaling (full lists are given in Supplementary Table 1). Looking more closely at the timing and processes of transcripts altered by GNRHR activation, it becomes clear that the changes classify into several distinct temporal and functional groups (Fig. 3). These patterns can be summarized as early sustained changes in transcription factors (EGR1, FosB, Fos EGR2, SRF, ATF3, and KLF6), G_1/S markers (MCM8 and CHEK2), and signaling apparatus – including regulators of inositol phosphate metabolism and MAP kinase phosphatases (DUSP5, DUSP1, INPP1, and ISYNA1); later and continuing changes in G_2/M markers (NDEL1, CDC2, TUBB4, DCTN1, KIF20A, CENPM, CENPF, and RASSF1A) and apoptotic apparatus (EIF5A, KLF10, BAX, and cFLAR); and more transient changes in cytoskeletal components

Figure 2

GNRH agonist causes significant changes in gene expression over 24 h. (A) The number of differentially expressed genes (Rank Products $P<0.05$) in SCL60 cells peaks 8 h after Triptorelin treatment, full lists of genes are in Supplementary Table 1. (B) The 25 most upregulated genes after Triptorelin treatment in SCL60 cells. (C) The 25 most downregulated genes after Triptorelin treatment in SCL60 cells (left), and the expression of these genes in the HEK293 Triptorelin-treated and untreated cells (right). Heatmaps represent changes in expression relative to the median of untreated SCL60 replicate cells (Red, upregulated; green, downregulated).

Table 1 Genes significantly increased and decreased with Triptorelin treatment in SCL60 cells were enriched for various signaling pathways. The predicted false discovery rate (FDR) and one-tail Fisher Exact test *P* values were calculated within DAVID. Highlighted genes (in bold) are among the 25 most increased or decreased probes (Fig. 2).

	Genes	*P* value	FDR
Increased pathways			
hsa04110: cell cycle	CDK1, ANAPC10P1, CDC14A, CDC14B, CCNH, ANAPC10, CCNE2, LOC440917, CCNB1, CDKN1A, YWHAG, MAD2L1, ORC6L, MDM2, CCNA1, GADD45B, MYC, GADD45A, BUB3	0.001	0.75
hsa04115: p53 signaling pathway	CCNE2, CCNB1, CDK1, CDKN1A, CASP9, RRM2, MDM2, PMAIP1, GADD45B, SESN2, THBS1, GADD45A	0.001	1.7
hsa04621: NOD-like receptor signaling pathway	MAP3K7, HSP90B1, **CCL2**, **IL8**, CXCL2, CCL8, NFKBIA, TRAF6, BIRC2, CHUK, CCL7	0.002	2.8
hsa04010: MAPK signaling pathway	MAPKAPK5, NFKB2, SRF, MAP3K7, **FOS**, DUSP14, JUND, MAP3K8, TRAF6, MYC, CHUK, RELB, ATF4C, **NR4A**1, FLNC, DDIT3, DUSP5, ATF4, DUSP3, DUSP1, RRAS2, LOC100133211, JUN, RAP1B, GADD45B, DUSP8, GADD45A	0.02	18
hsa04622: RIG-I-like receptor signaling pathway	MAP3K7, DDX3X, ISG15, **IL8**, IL12A, NFKBIA, TRAF6, CHUK, AZI2, TANK	0.02	20
Decreased pathways			
hsa04110: cell cycle	E2F2, LOC100133012, CDC14B, CREBBP, PRKDC, MCM2, CHEK2, MCM4, MCM5, LOC440917, RAD21, CDKN2A, EP300, MCM7, CDKN1B, CDKN2B, LOC646096, LOC731751, ABL1	5×10^{-4}	0.66
hsa04330: Notch signaling pathway	NOTCH3, CTBP1, NOTCH1, EP300, APH1A, CREBBP, JAG2, NCOR2	0.005	6.1
hsa04012: ErbB signaling pathway	LOC407835, CBLB, NRG4, CDKN1B, PAK2, PLCG1, ERBB3, MAP2K2, CAMK2G, PLCG2, ABL1	0.02	19
hsa04310: Wnt signaling pathway	WNT5A, FZD8, CTBP1, PPP2R5D, CAMK2G, CREBBP, VANGL2, FZD2, **FZD4**, CTNNBIP1, EP300, PRICKLE1, FRAT2, TBL1X	0.02	23
hsa04512: ECM-receptor interaction	SDC1, COL4A1, **LAMA5**, COL6A1, ITGB5, COL2A1, AGRN, COL4A6, HMMR	0.04	38

(TPM4, ITGAV, KIF5C, FLRT3, DSTN, MAPT, and DGCR2) and cyclins (CCNA1 and CGRRF1).

In order to establish whether the GNRHR-mediated gene expression changes observed were similar to GNRH-regulated changes in other systems, we compared them to a previous study by Kakar *et al.* (2003). These investigators reported a list of 68 genes whose expression was changed in mouse LβT2 gonadotrope cells following treatment with a GNRH agonist des-gly[10], [D-Ala[6]]-ethylamide GNRH. Human homologs could be identified for 59 of the mouse genes and these were sufficient to cluster the SCL60 dataset into treated and control groups. Of the 59 orthologous genes, 21 were commonly differentially expressed, including a number of the early response genes EGR1, FOSB, JUNB, and IER2 (Supplementary Table 1), although this study was limited to 1- and 24-h time points.

Dynamic phosphoproteomic response to GNRHR activation

Building upon the gene expression data, reverse-phase protein array (RPPA) technology was used as a screening tool to characterize the posttranscriptional response to GNRHR activation. The focus was on representative members of cell cycle components, growth regulators, MAPK signaling, and cell survival modulators, as these were suggested to be important from the gene expression data (Fig. 4A). Levels of pERK were increased, as expected from previous studies (Morgan *et al.* 2008) and levels of pNF-κB expression were also increased (Fig. 4B and C and Supplementary Figure 3, see section on supplementary data given at the end of this article). In contrast, pAkt decreased in a more gradual manner and pPTEN expression demonstrated a transient reduction (Fig. 4C and Supplementary Figure 3). The level of p-histone H3 showed a reduction initially but was increased after 24 h and may reflect cells accumulating in the G$_2$/M phase of the cell cycle. The overall reduction in pAkt and increases in the levels of pERK and pNF-κB expression were confirmed by western blot (Fig. 4B, C and D).

Triptorelin induces caspase-mediated apoptosis in SCL60 xenografts

We next assessed the effect of Triptorelin on GNRH signaling *in vivo*. Consistent with previous findings (Morgan *et al.* 2008), Triptorelin was found to cause a significant reduction in growth of SCL60 xenograft tumors, and we established that the GNRH agonist had no effect on
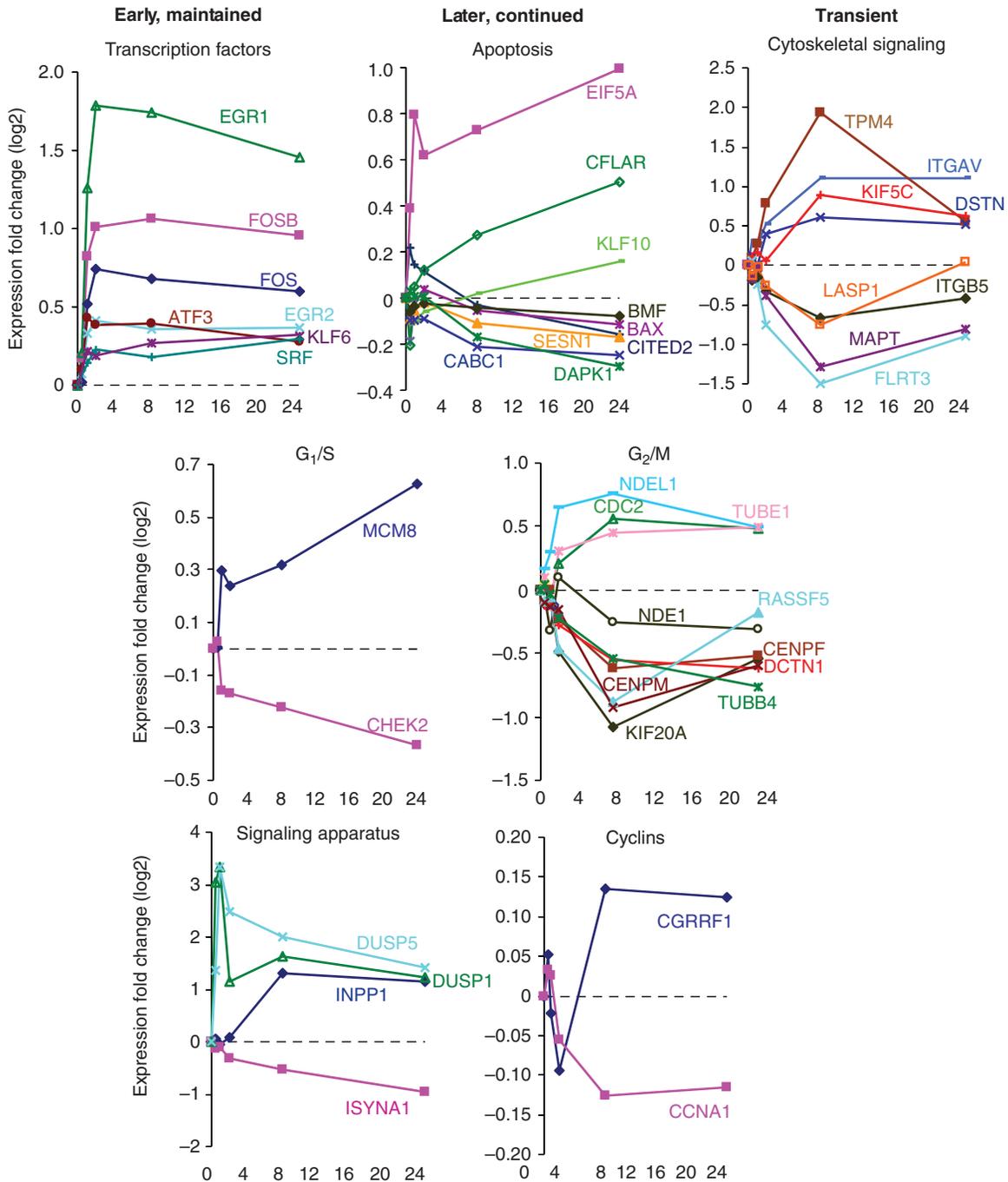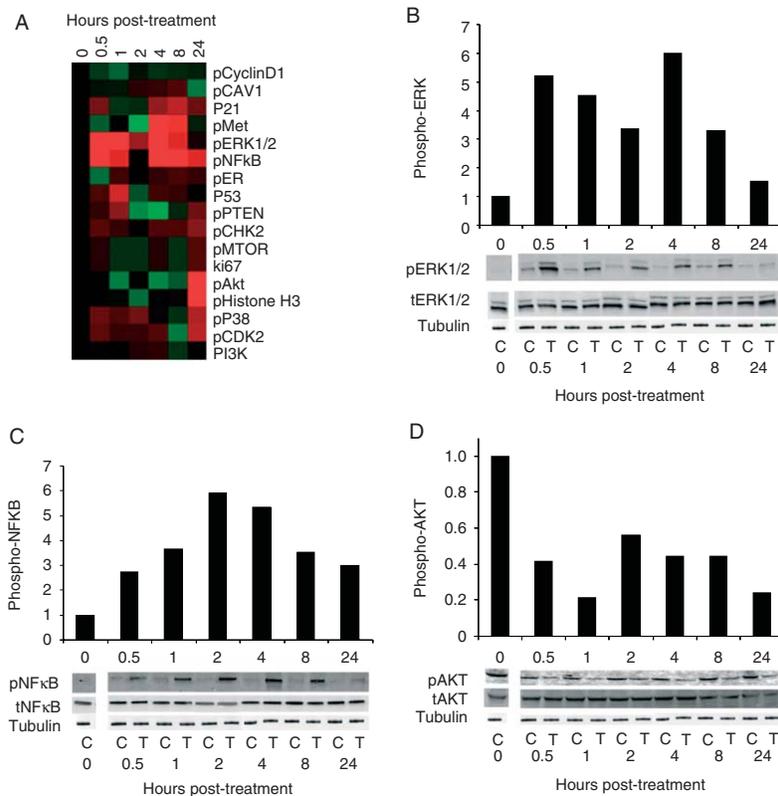
Figure 3

Temporal changes in the expression of genes in response to Triptorelin belong to different functional classes. Transcript expression can be tentatively classified into groups of 'early maintained', 'later, continued', or 'transient' changes in response to Triptorelin (upper panel). Changes in transcripts encoding components required in G_1/s, G_2/M, or cyclins and the signaling apparatus downstream from the GNRH receptor are also illustrated (middle and lower panels).

Figure 4

Reverse-phase protein array expression implicates changes in pERK, pAkt, and pNF-κB in the response to Triptorelin. (A) Changes in cancer-associated proteins following Triptorelin treatment for 0.5, 1, 2, 4, 8, and 24 h. Phosphoproteins are prefixed with lower case 'p' and their data are normalized to that of the corresponding total protein. Red, increased; Green, decreased. Changes in pERK1/2 (B), pNF-κB (C), and pAkt (D) were confirmed by western blot. Blots aligned below each time point are for control (left) and treated (right) respectively. Control and treated at the zero time point are the same. The increases in pERK and pNF-κB and decrease in pAKT observed in these individual western blots were also observed in parallel RPPA experiments (Supplementary Figure 3).

parental (HEK293) or mutated receptor-transfected (SCL215) cells (Fig. 5A). Immunostaining revealed decreased levels of p-Histone H3, consistent with reduced proliferation (Fig. 5B) and increased caspase 3, consistent with increased apoptosis following Triptorelin treatment for 4 and 7 days compared with untreated control tumors (Fig. 5B, $P = 0.004$). Representative images are shown in Supplementary Figure 2, see section on supplementary data given at the end of this article.

Phosphoproteomic profiling the response to Triptorelin in SCL60 xenograft tumors

To determine whether similar pathways were changed in response to a GNRH agonist *in vivo*, we used an antibody array with 117 pairs of antibodies (Supplementary Table 1) to detect both the phosphorylated and non-phosphorylated forms of selected proteins in SCL60 xenografts treated with Triptorelin. There were increases in phosphorylation of both NF-κB-p65 and IκBε after 4 days, consistent with the RPPA *in vitro* analysis and suggesting a possible involvement of the NF-κB survival signaling pathway in response to Triptorelin treatment. Also consistent with the RPPA data was the reduction in phosphorylated Akt at day 7. Changes observed in Chk2, p27, and CDC25C may be representative of the disruption to cell cycle progression. Dynamic changes in levels of phosphoproteins occurred: these included a gradual decrease in pMET, a transient increase in AMPK1, and a sustained increase in pMYC (Fig. 5C).

Inhibition of NF-κB enhances the anti-proliferative effect of GNRHR activation

As both *in vitro* RPPA and *in vivo* phosphoprotein array data highlighted that NF-κB signaling was activated in response

Published by Bioscientifica Ltd.

Endocrine-Related Cancer

to Triptorelin treatment, we investigated the *in vitro* gene expression patterns of several NF-κB pathway members in SCL60 cells following treatment with Triptorelin (Fig. 6A). NF-κB1 expression peaked at 8 h, whereas NF-κBIA and MAPK8 (an activator of NF-κB-p105) were highest after just 2 h, while gene expression levels of

IKBKG and IKBKB were largely unchanged. To validate the increase in pNF-κB seen upon GNRH stimulation *in vivo*, we next performed immunohistochemistry on the xenograft tumors and found pNF-κB to be significantly ($P=0.009$) higher following treatment with Triptorelin (Fig. 6B). Representative images are shown in
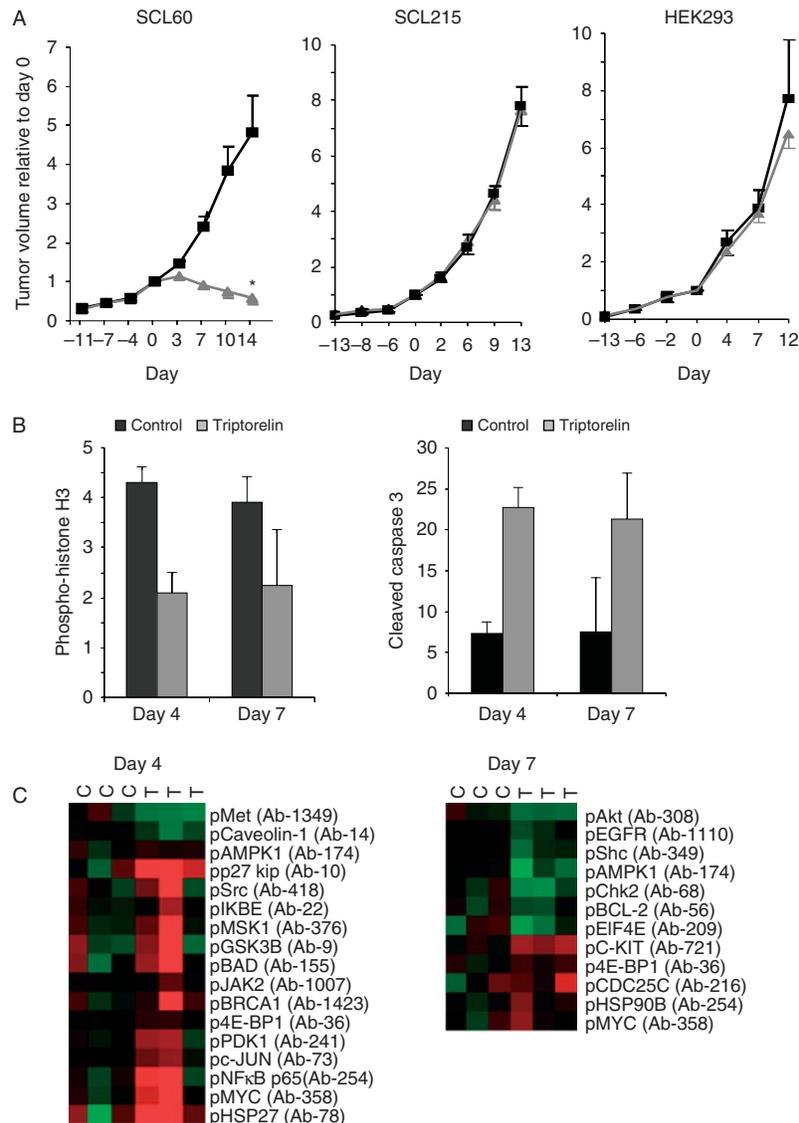

Figure 5

Triptorelin reduces tumor volume and proliferation while increasing apoptosis *in vivo*. Phosphoproteomic signaling highlights a number of pathways including NF-κB. (A) Tumor volume changes relative to day 0. Data are mean values of at least nine control xenograft tumors and nine Triptorelin-treated tumors. Error bars show ±s.e.m. 10 μg Triptorelin/mouse for up to 14 days. Initial tumor volumes at start of treatment were 73 (±11) mm³ for SCL60, 86 (±11) mm³ for SCL60, and 84 (±7) mm³ for HEK 293 xenografts. There was a reduction in proliferation, shown by phospho-

histone H3 (B), and an increase in apoptosis, shown by cleaved caspase 3 after 4 and 7 days. (C) Phosphoproteomic antibody arrays demonstrated changes in a number of phosphoproteins following Triptorelin treatment *in vivo* (Red, increased phosphorylation; Green, decreased phosphorylation); only those phosphoproteins that demonstrated a significant average increase/decrease at day 4 or 7 are shown. Closed black squares, Control; Closed grey triangle, Triptorelin.

Supplementary Figure 4, see section on supplementary data given at the end of this article.

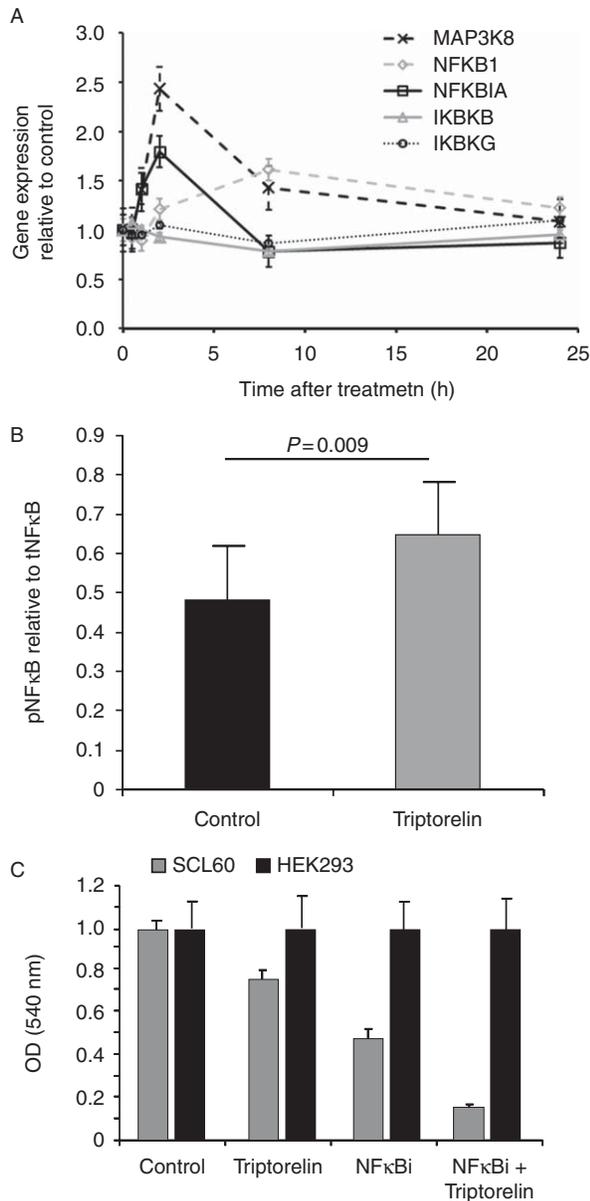To evaluate NF-κB signaling as a possible pathway to target in combination with GNRHR activation,

Figure 6

Inhibition of NF-κB enhances the anti-proliferative effect of GNRH receptor activation in HEK293 (SCL60). (A) The gene expression patterns of several NF-κB pathway members were increased in the short term following treatment with Triptorelin in SCL60 cells *in vitro*. (B) Immunohistochemistry of SCL60 xenograft tumors demonstrated a significant increase ($P=0.009$; *t*-test) in pNF-κB following treatment with Triptorelin. Eight control tumors were compared against nine triptorelin-treated tumors. (C) The NF-κB inhibitor, 15d-PGJ2 (NF-κB i), reduced growth of SCL60 cells and had an additive effect with Triptorelin.

we inhibited the pathway in SCL60 cells *in vitro*. After 4 days, we observed significant reduction of SCL60 cell growth when treated with either 100 nM Triptorelin or 3 μM 15d-PGJ$_2$ (NF-κB inhibitor) (Straus *et al.* 2000) and enhanced growth repression when both were used in combination (Fig. 6C), suggesting an additive effect. In contrast, none of these treatments influenced the growth of the parental HEK293 cells.

Discussion

Various G protein-coupled receptors (GPCRs) at the cell surface can influence cancer cell growth. Intense activation of the GNRHR, a Gq/11-coupled peptide hormone GPCR, can inhibit the proliferation of certain but not all cancer cell types. An improved understanding of how GNRH agonist anti-proliferative effects are elicited could address how certain cells are able to avoid the resulting downstream growth arrest signaling and treatment could be tailored more appropriately. Detailing the cellular responses to GPCR activation is a difficult process due to signaling pathway complexity and the temporal changes that occur downstream from receptor activation. In this study, we used global gene and protein expression approaches to explore GNRHR signaling in relation to cell growth inhibition. We identified a number of candidate signaling pathways that may be involved in mediating and modulating the direct anti-proliferative effect of GNRH agonists *in vitro* and *in vivo*. The transcriptional and proteomic changes observed suggest a model summarized in Fig. 7 where transcription factors are increased as an early response and maintained following Triptorelin treatment. Genes involved in apoptosis (e.g. *EIF5A* and *cFLAR*) and G$_1$/S transition signaling (e.g. *MCM8* and *CHEK2*) were altered in expression around 1–8 h after treatment, whereas expression of cytoskeletal (e.g. *TPM4*, *ITGAV*, *DSTN*, *MAPT* and *DGCR2*) and G$_2$/M-related (*NDEL1*, *CDC2* (*CDK1*), *TUBB4* (*TUBB4A*), *DCTN1*, *KIF20A*, *CENPM*, *CENPF*, *RASSF1A*) genes were changed around 8–24 h. The increased expression of early response genes such as FOS and EGR1 after 30 min to 1 or 2 h was consistent with previous observations of an intense and rapid increase in ERK phosphorylation immediately following GNRHR stimulation in SCL60 cells *in vitro* (Morgan *et al.* 2008), translocation to the nucleus, and the activation of these transcription factors. FOS gene family members encode proteins that dimerize with proteins of the JUN family to form the transcription factor complex AP-1 (Salisbury *et al.* 2008). The increased expression of both FOS and JUN
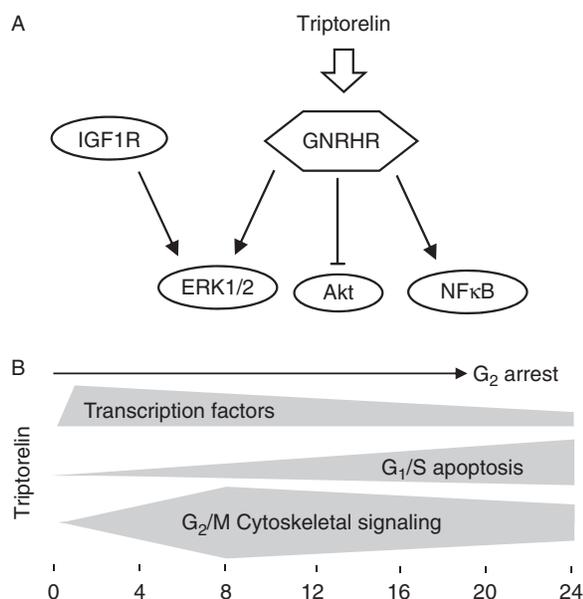
Figure 7

Model to summarize the anti-proliferative signaling response to a GNRH agonist. (A) Overview of the major downstream signaling pathways responding to Triptorelin identified by recent studies of transfected cells. (B) Preliminary model of temporal changes in gene expression following GNRH receptor activation in SCL60 cells indicating categories of genes such as transcription factor cell cycles and cytoskeletal components. The shape and volume of gray bars show approximate relative changes of gene transcript levels from different functional categories over 24 h.

family members make this a likely mechanism of transcriptional activation in SCL60 cells.

Flow cytometric analysis suggested that Triptorelin may induce G_2/M arrest and accumulation in S phase after 24 and 48 h. A number of cell cycle genes are differentially expressed, which may support this, particularly the increase in MAD2 mitotic arrest deficient-like 1 (MAD2L1), which encodes a protein that forms part of the spindle assembly checkpoint and prevents anaphase until chromosomes are properly aligned. Another component of the anaphase checkpoint, BUB3, was also increased (Taylor *et al.* 1998), along with the growth arrest and DNA-damage-inducible genes *GADD45A* and *GADD45B*. These genes have been shown to activate the p38/JNK pathway to cause G_2/M arrest (Zhu *et al.* 2009, Cho *et al.* 2010), and GADD45B has been shown to play a role in mediating Fas-induced apoptosis by enhancing the interaction between p38 and Rb (Cho *et al.* 2010). Several cell cycle-related proteins were also differentially phosphorylated: p27kip and CDC25C were increased, while Chk2 was decreased after 7 days. Changes in the

phosphorylation levels of the apoptosis regulators BCL2 and BAD were also observed.

Although ERK activation often drives proliferation, it has been associated with cell death in many different cell types (Zhuang & Schnellmann 2006, Mebratu & Tesfaigzi 2009). ERK-mediated G_2 arrest is thought to be dependent on PKC (Barboule *et al.* 1999, Dangi *et al.* 2006) and MEK1 (Dangi *et al.* 2006, Astuti *et al.* 2009). GNRHR signals through $G\alpha_q$ to activate PLCβ, causing PIP_2 cleavage and generation of DAG. IP_3 activates calcium channels in the endoplasmic reticulum to release Ca^{2+} and PKC is activated by DAG and Ca^{2+}. Once active, PKC phosphorylates Raf, which in turn activates MEK and downstream ERK. We have previously shown that the GNRHR-mediated anti-proliferative effect in SCL60 cells is dependent on PKC (Morgan *et al.* 2008). The ERK activation observed after Triptorelin treatment may be mediated through PKC and may be responsible for the G_2/M arrest observed in SCL60 cells.

Later-stage (8–24 h) gene expression changes reflected known GNRHR signaling effects exemplified by the CGA transcript, a stress response (IL8) and growth modulation (IGFBP5, FGFR, and Met). Changes in protein phosphorylation suggested modulation of membrane protein function (Cav-1), growth signaling (Met), metabolism (AMPK), cell motility (SRGAP3), and a pro-survival response (NF-κB). Clearly, the status of the cell cycle apparatus was altered with changes in p27, CDC25c, and Chk2.

NF-κB signaling was highlighted by both *in vivo* and *in vitro* approaches; the additive effect of Triptorelin plus 15d-PGJ(2) on growth inhibition may represent a useful target for drug combination treatments. Triptorelin has previously been shown to induce NF-κB activation in ovarian cancer cells (EFO-21 and EFO-27), which inhibited doxorubicin-induced apoptosis (Grundker *et al.* 2000). As 15d-PGJ(2) elicits effects via PPAR-gamma and NF-κB, the effect on growth in combination with Triptorelin may be somewhat cell type specific. This phenomenon will require further investigation. The results of the current study indicate the intricacy of the regulatory response to GNRHR activation. We found good agreement between our gene expression data and a previous study of gene expression changes in mouse LβT2 gonadotrope cells following treatment with a GNRH agonist (Kakar *et al.* 2003). However, our recent findings that the overexpression of GNRHR alone is not sufficient to facilitate an anti-proliferative response to Triptorelin in several breast cancer cell lines (Morgan *et al.* 2011*b*) provides an excellent opportunity to interrogate the factors and mechanisms involved in cell-type-specific differences

that mediate the direct anti-proliferative effect of GNRH agonists. These may entail analyses of the changes occurring in WPE-1-NB26 cells, which exhibit cell cycle arrest without prominent commitment to apoptosis and manipulation of gene expression in MCF-7 cells, which escape GNRHR-mediated growth inhibition.

In conclusion, *in vitro* and *in vivo* transcriptomic and proteomic approaches were used to characterize the anti-proliferative effects of a GNRH agonist at the molecular signaling level. The anti-proliferative response induced by GNRHR activation appears to result in apoptosis and G_2/M arrest mediated via a coordinated dynamic pattern of MAPK, cell cycle, apoptotic, and cytoskeletal-related signaling. Key regulators pAKT and pERK were repressed and induced respectively, while pNF-κB was activated and may represent a useful target for enhancing this intriguing anti-proliferative response.

References

Acharya CR, Hsu DS, Anders CK, Anguiano A, Salter KH, Walters KS, Redman RC, Tuchman SA, Moylan CA, Mukherjee S *et al.* 2008 Gene expression signatures, clinicopathological features, and individualized therapy in breast cancer. *Journal of the American Medical Association* **299** 1574–1587. (doi:10.1001/jama.299.13.1574)

Angelucci C, Iacopino F, Lama G, Capucci S, Zelano G, Boca M, Pistilli A & Sica G 2004 Apoptosis-related gene expression affected by a GnRH analogue without induction of programmed cell death in LNCaP cells. *Anticancer Research* **24** 2729–2738.

Astuti P, Pike T, Widberg C, Payne E, Harding A, Hancock J & Gabrielli B 2009 MAPK pathway activation delays G_2/M progression by destabilizing Cdc25B. *Journal of Biological Chemistry* **284** 33781–33788. (doi:10.1074/jbc.M109.027516)

Barboule N, Lafon C, Chadebech P, Vidal S & Valette A 1999 Involvement of p21 in the PKC-induced regulation of the G_2/M cell cycle transition. *FEBS Letters* **444** 32–37. (doi:10.1016/S0014-5793(99)00022-8)

Blankenstein MA, Henkelman MS & Klijn JG 1985 Direct inhibitory effect of a luteinizing hormone-releasing hormone agonist on MCF-7 human breast cancer cells. *European Journal of Cancer & Clinical Oncology* **21** 1493–1499. (doi:10.1016/0277-5379(85)90244-5)

Breitling R, Armengaud P, Amtmann A & Herzyk P 2004 Rank products: a simple, yet powerful, new method to detect differentially regulated genes in replicated microarray experiments. *FEBS Letters* **573** 83–92. (doi:10.1016/j.febslet.2004.07.055)

Cho HJ, Park SM, Hwang EM, Baek KE, Kim IK, Nam IK, Im MJ, Park SH, Bae S, Park JY *et al.* 2010 Gadd45b mediates Fas-induced apoptosis by enhancing the interaction between p38 and retinoblastoma tumor suppressor. *Journal of Biological Chemistry* **285** 25500–25505. (doi:10.1074/jbc.M109.091413)

Dangi S, Chen FM & Shapiro P 2006 Activation of extracellular signal-regulated kinase (ERK) in G_2 phase delays mitotic entry through p21CIP1. *Cell Proliferation* **39** 261–279. (doi:10.1111/j.1365-2184.2006.00388.x)

Dunning MJ, Smith ML, Ritchie ME & Tavare S 2007 beadarray: R classes and methods for Illumina bead-based data. *Bioinformatics* **23** 2183–2184. (doi:10.1093/bioinformatics/btm311)

Eidne KA, Flanagan CA, Harris NS & Millar RP 1987 Gonadotropin-releasing hormone (GnRH)-binding sites in human breast cancer cell lines and inhibitory effects of GnRH antagonists. *Journal of Clinical Endocrinology and Metabolism* **64** 425–432. (doi:10.1210/jcem-64-3-425)

Emons G, Pahwa GS, Brack C, Sturm R, Oberheuser F & Knuppen R 1989 Gonadotropin releasing hormone binding sites in human epithelial ovarian carcinomata. *European Journal of Cancer & Clinical Oncology* **25** 215–221. (doi:10.1016/0277-5379(89)90011-4)

Emons G, Schroder B, Ortmann O, Westphalen S, Schulz KD & Schally AV 1993a High affinity binding and direct antiproliferative effects of luteinizing hormone-releasing hormone analogs in human endometrial cancer cell lines. *Journal of Clinical Endocrinology and Metabolism* **77** 1458–1464. (doi:10.1210/jc.77.6.1458)

Emons G, Ortmann O, Becker M, Irmer G, Springer B, Laun R, Holzel F, Schulz KD & Schally AV 1993b High affinity binding and direct antiproliferative effects of LHRH analogues in human ovarian cancer cell lines. *Cancer Research* **53** 5439–5446.

Emons G, Grundker C, Gunthert AR, Westphalen S, Kavanagh J & Verschraegen C 2003 GnRH antagonists in the treatment of gyneco-logical and breast cancers. *Endocrine-Related Cancer* **10** 291–299. (doi:10.1677/erc.0.0100291)

Finch AR, Green L, Hislop JN, Kelly E & McArdle CA 2004 Signaling and antiproliferative effects of type I and II gonadotropin-releasing hormone receptors in breast cancer cells. *Journal of Clinical Endocrinology and Metabolism* **89** 1823–1832. (doi:10.1210/jc.2003-030787)

Gentleman RC, Carey VJ, Bates DM, Bolstad B, Dettling M, Dudoit S, Ellis B, Gautier L, Ge Y, Gentry J *et al.* 2004 Bioconductor: open software development for computational biology and bioinformatics. *Genome Biology* **5** R80. (doi:10.1186/gb-2004-5-10-r80)

Grundker C, Schulz K, Gunthert AR & Emons G 2000 Luteinizing hormone-releasing hormone induces nuclear factor kappaB-activation and inhibits apoptosis in ovarian cancer cells. *Journal of Clinical Endocrinology and Metabolism* **85** 3815–3820. (doi:10.1210/jc.85.10.3815)

Grundker C, Volker P & Emons G 2001 Antiproliferative signaling of luteinizing hormone-releasing hormone in human endometrial and ovarian cancer cells through G protein alpha(I)-mediated activation of phosphotyrosine phosphatase. *Endocrinology* **142** 2369–2380. (doi:10.1210/en.142.6.2369)

Grundker C, Gunthert AR, Millar RP & Emons G 2002 Expression of gonadotropin-releasing hormone II (GnRH-II) receptor in human endometrial and ovarian cancer cells and effects of GnRH-II on tumor cell proliferation. *Journal of Clinical Endocrinology and Metabolism* **87** 1427–1430. (doi:10.1210/jc.87.3.1427)

Huang da W, Sherman BT & Lempicki RA 2009 Systematic and integrative analysis of large gene lists using DAVID bioinformatics resources. *Nature Protocols* **4** 44–57. (doi:10.1038/nprot.2008.211)

Published by Bioscientifica Ltd.

Ihaka R & Gentleman R 1996 R: a language for data analysis and graphics. *Journal of Computational and Graphical Statistics* **5** 299–314. (doi:10.2307/1390807)

Kakar SS, Winters SJ, Zacharias W, Miller DM & Flynn S 2003 Identification of distinct gene expression profiles associated with treatment of LbetaT2 cells with gonadotropin-releasing hormone agonist using microarray analysis. *Gene* **308** 67–77. (doi:10.1016/S0378-1119(03)00446-3)

Kononen J, Bubendorf L, Kallioniemi A, Barlund M, Schraml P, Leighton S, Torhorst J, Mihatsch MJ, Sauter G & Kallioniemi OP 1998 Tissue microarrays for high-throughput molecular profiling of tumor specimens. *Nature Medicine* **4** 844–847. (doi:10.1038/nm0798-844)

Limonta P, Dondi D, Moretti RM, Maggi R & Motta M 1992 Antiproliferative effects of luteinizing hormone-releasing hormone agonists on the human prostatic cancer cell line LNCaP. *Journal of Clinical Endocrinology and Metabolism* **75** 207–212. (doi:10.1210/jc.75.1.207)

Limonta P, Marelli MM, Mai S, Motta M, Martini L & Moretti RM 2012 GnRH receptors in cancer: from cell biology to novel targeted therapeutic strategies. *Endocrine Reviews* **33** 784–811. (doi:10.1210/er.2012-1014)

Marini L, Iacopino F, Schinzari G, Robustelli della Cuna FS, Mantovani G & Sica G 1994 Direct antiproliferative effect of triptorelin on human breast cancer cells. *Anticancer Research* **14** 1881–1885.

Maudsley S, Davidson L, Pawson AJ, Chan R, Lopez de Maturana R & Millar RP 2004 Gonadotropin-releasing hormone (GnRH) antagonists promote proapoptotic signaling in peripheral reproductive tumor cells by activating a Galphai-coupling state of the type I GnRH receptor. *Cancer Research* **64** 7533–7544. (doi:10.1158/0008-5472.CAN-04-1360)

Mebratu Y & Tesfaigzi Y 2009 How ERK1/2 activation controls cell proliferation and cell death: is subcellular localization the answer? *Cell Cycle* **8** 1168–1175. (doi:10.4161/cc.8.8.8147)

Miller WR, Scott WN, Morris R, Fraser HM & Sharpe RM 1985 Growth of human breast cancer cells inhibited by a luteinizing hormone-releasing hormone agonist. *Nature* **313** 231–233. (doi:10.1038/313231a0)

Moretti RM, Marelli MM, Dondi D, Poletti A, Martini L, Motta M & Limonta P 1996 Luteinizing hormone-releasing hormone agonists interfere with the stimulatory actions of epidermal growth factor in human prostatic cancer cell lines, LNCaP and DU 145. *Journal of Clinical Endocrinology and Metabolism* **81** 3930–3937. (doi:10.1210/jc.81.11.3930)

Morgan K, Stewart AJ, Miller N, Mullen P, Muir M, Dodds M, Medda F, Harrison D, Langdon S & Millar RP 2008 Gonadotropin-releasing hormone receptor levels and cell context affect tumor cell responses to agonist *in vitro* and *in vivo*. *Cancer Research* **68** 6331–6340. (doi:10.1158/0008-5472.CAN-08-0197)

Morgan K, Stavrou E, Leighton SP, Miller N, Sellar R & Millar RP 2011a Elevated GnRH receptor expression plus GnRH agonist treatment inhibits the growth of a subset of papillomavirus 18-immortalized human prostate cells. *Prostate* **71** 915–928. (doi:10.1002/pros.21308)

Morgan K, Meyer C, Miller N, Sims AH, Cagnan I, Faratian D, Harrison DJ, Millar RP & Langdon SP 2011b GnRH receptor activation competes at a low level with growth signaling in stably transfected human breast cell lines. *BMC Cancer* **11** 476. (doi:10.1186/1471-2407-11-476)

Salisbury TB, Binder AK & Nilson JH 2008 Welcoming β-catenin to the gonadotropin-releasing hormone transcriptional network in gonadotropes. *Molecular Endocrinology* **22** 1295–1303. (doi:10.1210/me.2007-0515)

Skehan P, Storeng R, Scudiero D, Monks A, McMahon J, Vistica D, Warren JT, Bokesch H, Kenney S & Boyd MR 1990 New colorimetric cytotoxicity assay for anticancer-drug screening. *Journal of the National Cancer Institute* **82** 1107–1112. (doi:10.1093/jnci/82.13.1107)

Spurrier B, Ramalingam S & Nishizuka S 2008 Reverse-phase protein lysate microarrays for cell signaling analysis. *Nature Protocols* **3** 1796–1808. (doi:10.1038/nprot.2008.179)

Straus DS, Pascual G, Li M, Welch JS, Ricote M, Hsiang CH, Sengchanthalangsy LL, Ghosh G & Glass CK 2000 15-Deoxy-delta 12,14-prostaglandin J2 inhibits multiple steps in the NF-kappa B signaling pathway. *PNAS* **97** 4844–4849. (doi:10.1073/pnas.97.9.4844)

Taylor SS, Ha E & McKeon F 1998 The human homologue of Bub3 is required for kinetochore localization of Bub1 and a Mad3/Bub1-related protein kinase. *Journal of Cell Biology* **142** 1–11. (doi:10.1083/jcb.142.1.1)

White CD, Coetsee M, Morgan K, Flanagan CA, Millar RP & Lu ZL 2008 A crucial role for Galphaq/11, but not Galphai/o or Galphas, in gonadotropin-releasing hormone receptor-mediated cell growth inhibition. *Molecular Endocrinology* **22** 2520–2530. (doi:10.1210/me.2008-0122)

Zhu N, Shao Y, Xu L, Yu L & Sun L 2009 Gadd45-alpha and Gadd45-gamma utilize p38 and JNK signaling pathways to induce cell cycle G_2/M arrest in Hep-G_2 hepatoma cells. *Molecular Biology Reports* **36** 2075–2085. (doi:10.1007/s11033-008-9419-9)

Zhuang S & Schnellmann RG 2006 A death-promoting role for extracellular signal-regulated kinase. *Journal of Pharmacology and Experimental Therapeutics* **319** 991–997. (doi:10.1124/jpet.106.107367)